IEEE Access
Multidisciplinary | Rapid Review | Open Access Journal

Received December 17, 2019, accepted January 4, 2020, date of publication January 20, 2020, date of current version January 31, 2020.

Digital Object Identifier 10.1109/ACCESS.2020.2968060

Low-Profile Aperture-Coupled Patch Antenna Array for CubeSat Applications

PATRÍCIA BOUÇA[1], (Member, IEEE), JOÃO NUNO MATOS[1], (Member, IEEE), SÉRGIO REIS CUNHA[2], AND NUNO BORGES CARVALHO[1], (Fellow, IEEE)

[1]Departamento de Eletrónica, Telecomunicações e Informática, Instituto de Telecomunicações, Universidade de Aveiro, 3810-193 Aveiro, Portugal
[2]Departamento de Engenharia Eletrotécnica e de Computadores, Faculdade de Engenharia, Universidade do Porto, 4200-465 Porto, Portugal

Corresponding author: Patrícia Bouça (patricia.bouca@ua.pt)

This work was supported in part by the European Regional Development Fund (FEDER), through the Regional Operational Programme of Lisbon (POR LISBOA 2020), and in part by the Competitiveness and Internationalization Operational Programme through COMPETE 2020 of the Portugal 2020 framework, Project INFANTE, under Grant 024534 and Grant POCI-01-0247-FEDER-024534.

ABSTRACT This paper presents the design, simulation, and measurement results of a dual aperture-coupled microstripline-fed antenna array with circular polarization at the C-band for small satellites applications. The antenna array was designed at a center frequency of 5.5 GHz, and it has a two-port isolation bandwidth of 25 MHz above 20 dB while the axial ratio is below 1 dB. The main objective is to produce a four-patch antenna array to be mounted on CubeSat deployable wings along with a layer of solar panels, maximizing the usable space and obtaining a better link budget for a standardized Cubesat of 10 cm × 10 cm × 10 cm. The orthogonal feedlines' isolation between Tx/Rx signals and a minimization of the multi-layer design provide a lower profile approach considering the state-of-the-art. The significant thickness reduction combined with a new perspective of having both deployable wings transmitting and receiving signals lead to a notable improvement of the overall system. This work is relevant due to the demand for high-performance antenna systems that may expand the capabilities of CubeSats, considering the importance of using an antenna array instead of a single element approach.

INDEX TERMS Antenna array, circular polarization, CubeSats, small satellites.

I. INTRODUCTION

Since the last decade, small satellites technology has evolved rapidly providing opportunities to universities and commercial launches with academic and research motivations. The key member of the small satellite family is the CubeSat. This type of satellites hit a perfect balance between cost, mission lifetime, and payload opportunities. One of the potential applications of these satellites is Earth observation, that can be used when the satellite is equipped with a Surface Aperture Radars (SAR) payload. These SAR solutions impose that the satellite payload includes a high-performance antenna system. These antenna systems in CubeSat's are actually one of the most challenging problems due to the relationship between miniaturization and antenna performance [1]–[4].

This work is devoted to the antenna design that can cope with high performance for SAR applications, but with a limited size of the satellite. The antenna array was designed to be installed on a CubeSat with several flat panels covered on one side by solar panels and the other side by the radiating elements, Fig. 1. With a star tracker measuring the satellite location, the momentum wheels are used to guarantee stability and control over the three axes. The most critical issues regarding the design are the reduction of volume and mass, guaranteeing that the potential of the available space is exploited to its maximum. The proposed configuration avoids the usage of a circulator to separate Tx/Rx, which is typically quite expensive, and its design implies a significant volume and space on the flat panel, Fig. 2.

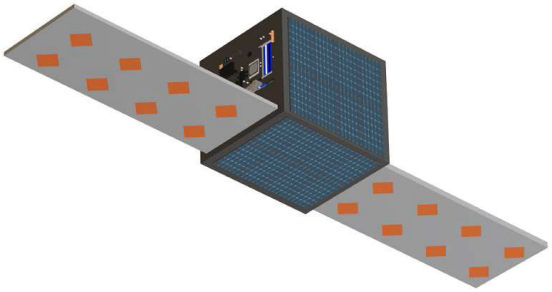

FIGURE 1. CubeSat representation.

The associate editor coordinating the review of this manuscript and approving it for publication was Mohammad Tariqul Islam.

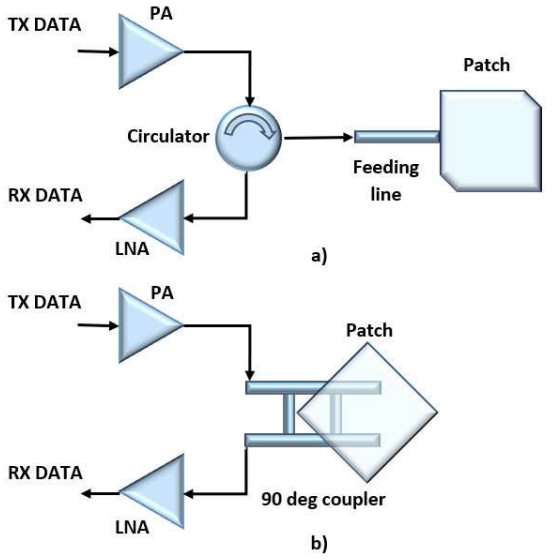

FIGURE 2. Communication systems representation: (a) Usage of a circulator component to separate the transmitting and receiving signals, (b) Circulator avoidance to separate the transmitting and receiving signals.

The key advantage of developing an approach that ensures a more efficient usage of the antenna system is the better payload and link budget that the system may provide [5]–[8].

Different solutions for the development of antenna arrays have been discussed and one of the most versatile elements is the microstrip patch antenna because not only it can be integrated with solar panels, but it also can be used as TX and RX in only one array, on two separated arrays or even as feed for a reflectarray [3], [4].

For the purpose of combining an high gain antenna array and minimize layers' thickness, several antenna designs were explored.

In [6], [9]–[12], there is frequent usage of multilayer circular polarization (CP) patch antennas which may come with several advantages, such as, not requiring a precise orientation between transmitting and receiving antennas, and the narrow beamwidth that is very important to communicate with high-orbital satellites. However, in various implementations, there is constant utilization of foam, in some cases, Rohacell foam, placed between the top (patch antenna) and the bottom layers, or between the feed layers and an air layer, so the radiating element is suspended [10]–[13]. It was also addressed the issue of obtaining dual-polarization using a single patch antenna with different configurations. To the best of our knowledge, the most relevant publication accounting for the isolation between ports placed in the same CP patch antenna is presented in [10]. Although this implementation guarantees a broader bandwidth of isolation, the design has four times more thickness when compared to the one presented in this work. The usage of multiple layers may compromise the integration of the antenna in the CubeSat flat panels along with the solar cells due to the increase of thickness and weight [9]–[11]. These referenced implementations do not propose an arrangement of an antenna array and, as a consequence, the capabilities of an innovative arrangement are not fully explored. A revision of the metrics compared in this work with the work presented in the state of the art is presented in Table 1.

TABLE 1. CP antennas state-of-the-art.

Ref	Antenna Thickness (mm)	Center Frequency (GHz)	Isolation (dB)
[9]	> 3.2	3.15 and 2.454	5 to 10
[10]	> 6	5.8	28
[11]	> 6.5	2	no information
[12]	3.5	19	20 to 25
[13]	> 3.2	0.9	25
This work	1.63	5.5	> 20

The final challenge of the panel construction from the RF point of view is the transmitter due to the high-power density components, such as Power Amplifiers (PAs), so a more reliable power dissipation structure must be developed. Typically, an aluminum structure is fixed to the overall board between the radiating elements and the solar panels, directing the heat to space [14]. The antenna array proposed in this work was designed to operate according to the International Telecommunication Union (ITU) standards allocated range for the Earth exploration-satellite service (EESS) (active) and space research service (5.25 - 5.57 GHz). This band was selected to Earth exploration-satellite and space research (both active) flying at an altitude of 785-800 km [15]. The novelty of this work is the integration of an antenna array with a thickness of less than 1.6 *mm* into a CubeSat that guarantees the potential of having all the panels for transmitting and receiving signals using the same elements while existing isolation between both ports of the antenna. This isolation is essential to protect the other RF components which are crucial to the success of the transmitting and receiving systems, such as, Low Noise Amplifiers (LNA) and PA.

II. APERTURE COUPLED PATCH ANTENNA DESIGN

A. ANTENNA DESIGN

The configuration of the circular polarization aperture coupled microstrip patch antenna is presented in Fig. 3. The antenna consists of a two-layer substrate of Astra MT77 laminate material ($\epsilon_r = 3$, $tan\delta = 0.0017$, $h = 0.762mm$) on which a square patch antenna is placed, and the feeding network is performed with a hybrid coupler. The implementation and design of the structure were performed in CST Microwave Design Studio.

The aperture coupled patch antenna was the selected geometry to reduce the radiation from the feed network that can interfere with the main radiation pattern. The ground plane separates the direct connection between them, and the slot is smaller than resonant size, so it is guaranteed that the radiation mainly comes from the resonant patch element [16], [17].

Assuming the patch antenna resonates at its dominant mode, the approximation of the fields inside the cavity formed by the patch and the magnetic walls around the

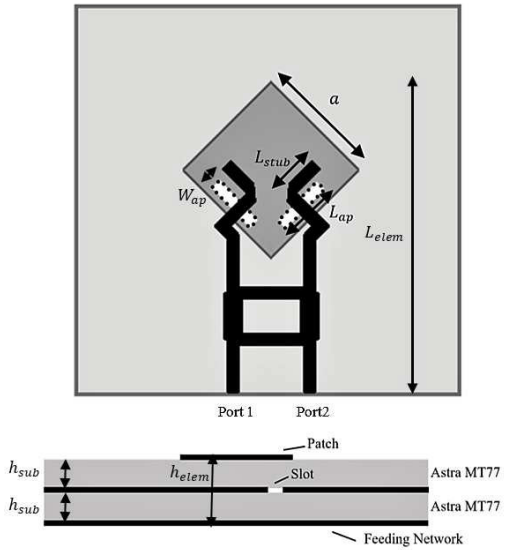

FIGURE 3. Antenna geometry with fixed parameters: $a = 14.72$ *mm*, $W_{ap} = 1.34$ *mm*, $L_{elem} = 47.61$ *mm*, $h_{sub} = 0.762$ *mm*, $h_{elem} = 1.63$ *mm*.

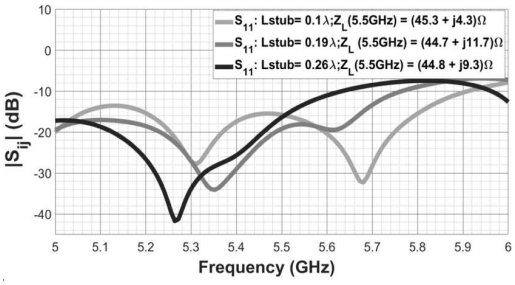

FIGURE 4. $|S_{11}|$ simulation results as a function of the stub length.

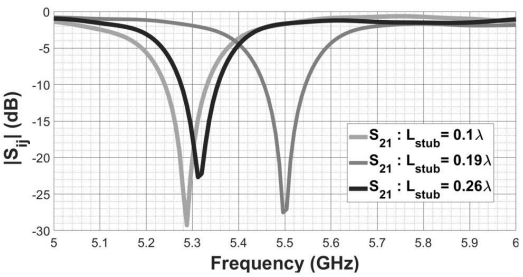

FIGURE 5. $|S_{21}|$ simulation results as a function of the stub length.

periphery of itself are expressed in [17] by:

$$E_z(x) = \frac{k_0^2}{j\omega\varepsilon_0} cos(\frac{\pi x}{a}) \tag{1}$$

$$H_y(x) = \frac{\pi}{a} sin(\frac{\pi x}{a}) \tag{2}$$

where a is the antenna resonant dimension, $k_0 = 2\pi/\lambda_0$, and it will depend on the position of the aperture located on its line segment. To have the same coupling coefficients between the cavity fields and the feedlines, the fields inside the two cavities must be equal, and that is only obtained if the patch antenna is a square of dimensions axa.

According to [18], the approximation of first order to the fields under the feedlines, considering an infinitely long microstrip line is given by:

$$E_z = e^{-jk} e^x \tag{3}$$

$$H_y = \frac{h_{sub}}{WZ_c} e^{-jk} e^x \tag{4}$$

where k is the effective propagation constant of the line, h_{sub} is the feedline substrate thickness, W is the 50Ω line width, and Z_c is the characteristic impedance of the line, 50Ω. Taking this approximation into consideration, the fields under the feedlines increase exponentially with the offset to the center of the antenna, x_0, so the line width has to be the same for both feedlines to maintain the same fields under themselves.

The coupling coefficients between the cavity fields and the feedlines can also be obtained with the following:

$$C_P = \frac{\frac{2}{3} r_0^3 \varepsilon_{r1} k_0^2}{P_{10}} cos(\frac{\pi x_0}{a}) \tag{5}$$

$$C_M = \frac{-jk_0 Z_0 \frac{4}{3} r_0^3 (\frac{\pi d}{aW})}{P_{10} Z_c} sin(\frac{\pi x_0}{a}) \tag{6}$$

where C_P and C_M denote the coupling factors via electric dipole and magnetic dipole coupling, respectively [17]. The coupling coefficients between the cavity fields designed in this microstrip patch antenna are equal when: the cavities have the same length and width, W; they are positioned with the same offset related to the center, x_0; they have the same radius,r_0, total power flow, P_10, and antenna resonant dimension, a. According to [16], if the cavity is rectangular the dependence will be equally relevant but in function of the aperture and width length of the slot, in which the reduction of the aperture length decreases the coupling factor. This behavior leads to the conclusion that the antenna should have linear polarization, and the 90 deg hybrid coupler (external element to be included) will be the only one to influence the patch antenna polarization. This can only be taken into consideration if the two feedlines are under identical conditions as it is described above. The most important combination of methods for the development of this implementation was the feed network design and the radiating element configuration, widely related to the slot aperture and stub length, to obtain the desired return loss and guarantee isolation above 20 dB. So, for this solution, it is proposed an alternative placement of the coupling slots to ensure that due to the increasing of the frequency and consequently reduction of the patch size, it is possible to obtain the desired metrics.

B. STUB AND APERTURE LENGTH

In this section, the antenna impedance is compared as a function of stub length and aperture length considering that the orthogonal feedlines should have isolation Tx/Rx, so that the area available for both polarizations is the highest possible.

The scattering parameters are presented according to [19]. The results presented in Fig. 4 demonstrate the effect of the various feedline stub length adjusted to have the desired reactance. Although the best situation would be obtaining a null reactance, the antenna design also considered the isolation

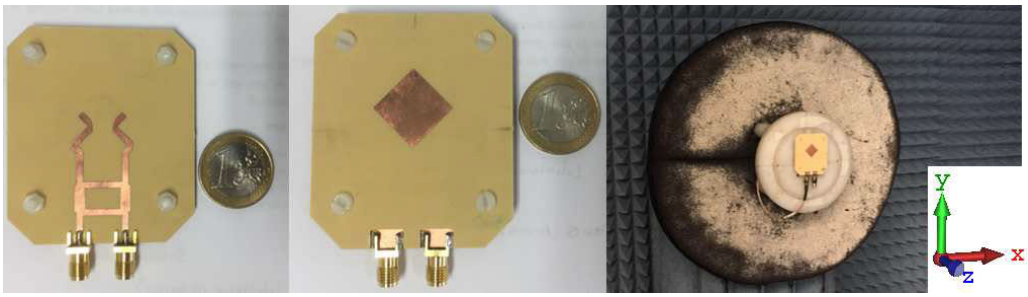

FIGURE 6. Fabricated antenna element and anechoic chamber measurement environment.

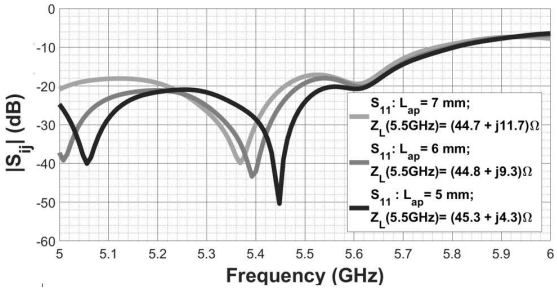

FIGURE 7. $|S_{11}|$ simulation results as a function of the aperture length ($L_{stub} = 0.19\lambda_{5.5GHz}$).

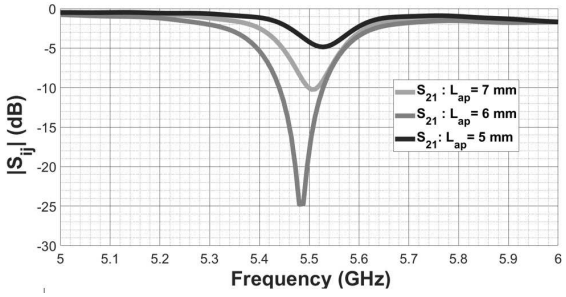

FIGURE 8. $|S_{21}|$ simulation results as a function of the aperture length ($L_{stub} = 0.19\lambda_{5.5GHz}$).

between Port 1 and Port 2, Fig. 5. Due to this, a compromise had to be made regarding all the desired parameters. This stub should have a close length according to the one recommended in [17]. In Fig. 7, the aperture length of the slot was varied to obtain a result for the impedance close to 50Ω and as it was done previously, considering the isolation between Port 1 and Port 2, Fig. 8.

C. RETURN LOSS AND ISOLATION

As it is reported in [16] and [17], the substrate thickness is one of the most influential parameters to manipulate the coupling effects between the feedlines and the antenna. During this work, a trade-off between the material thickness and the isolation between ports of the developed antenna was thought along with the design because the same center frequency is used to Tx/Rx signals without investing in a dual-band approach.

The open-circuited tuning stub cancels the normalized reactance at 5.5 GHz with $0.19\lambda_{5.5GHz}$ and the desired 50Ω is obtained. The chosen values for the stub and aperture length

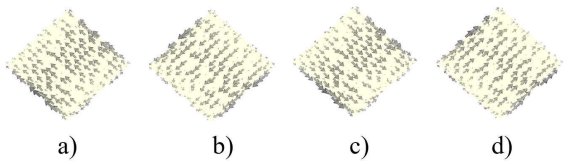

FIGURE 9. Radiating surface current distribution of the patch antenna Port 1 in phase intervals from: a) 0 deg b) 90 deg c) 180 deg d) 270 deg.

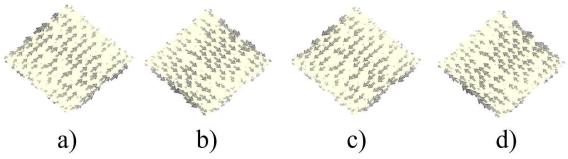

FIGURE 10. Radiating surface current distribution of the patch antenna Port 2 in phase intervals from: a) 0 deg b) 90 deg c) 180 deg d) 270 deg.

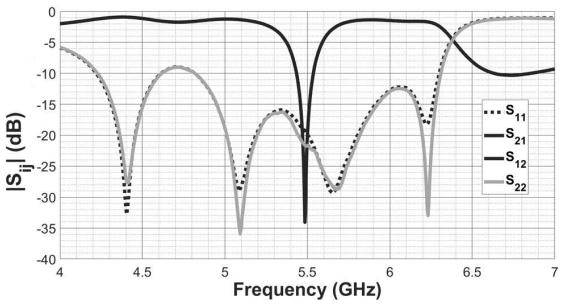

FIGURE 11. $|S_{ij}|$ measurement results for $L_{stub} = 0.19\lambda_{5.5GHz}$ and $L_{ap} = 4\ mm$.

were $0.19\lambda_{5.5GHz}$ and $5mm$ respectively because of the best isolation obtained between ports.

D. SURFACE CURRENT DISTRIBUTION

The surface current distribution at 5.5 GHz on the feedlines are presented in Fig. 9 and 10. The two different paths (clockwise: Tx port; counterclockwise: Rx port) show the high attenuation and the isolation between Tx/Rx signals. The current distribution on the radiating element at 5.5 GHz is also presented in four phase frames.

As it is presented in Fig. 9, by selecting Port 1 as Tx and Port 2 as Rx, the current vector causes RHCP (clockwise). In Fig. 10, the LHCP (counterclockwise) is achieved by symmetrically exciting the element. The analysis of the presented results outlines the capacity of the single element to have a CP and isolation between the Tx/Rx signals.

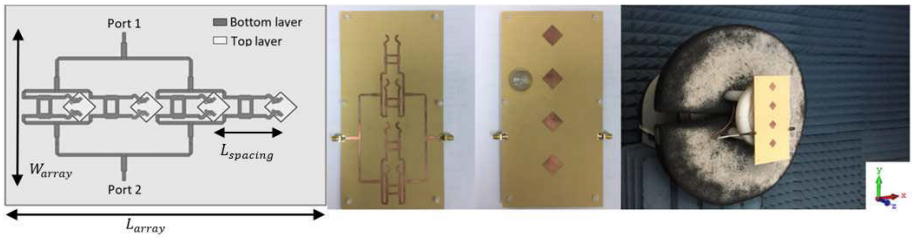

FIGURE 12. Antenna array geometry and fabricated and anechoic chamber environment ($L_{array} = 230\ mm$, $W_{array} = 105\ mm$ and $L_{spacing} = 45.45\ mm$).

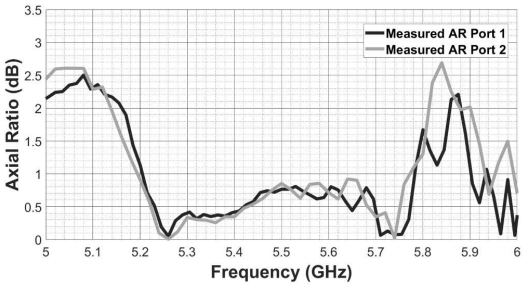

FIGURE 13. Axial Ratio exciting Port 1 and Port 2 alternatively.

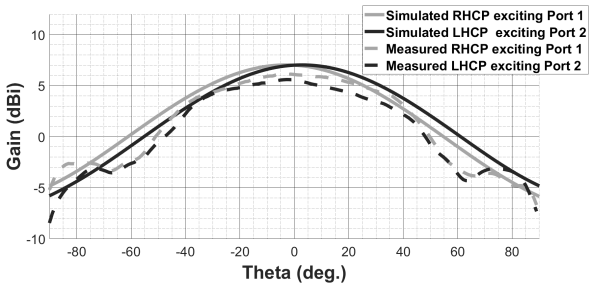

FIGURE 14. Simulation and Measurement results of the antenna radiation pattern showing 5.1-dBi gain at 5.5GHz for the CP mode of the antenna element.

III. SINGLE PATCH ANTENNA MEASUREMENT RESULTS

The proposed antenna simulated results were validated with impedance and radiation characteristics measurements using Keysight PNA-X N5224A network analyzer, Keysight VNA ZVB20 network analyzer, and an anechoic chamber, respectively.

A. RETURN LOSS AND ISOLATION

The measurement results presented in Fig. 11 involved adjustments in the patch size (addition of 0.4 *mm*) due to slight differences between measured and simulation results.

The isolation bandwidth between Port 1 and Port 2 above 20 dB was 31 MHz (5.47 - 5.51 GHz). The respective band is included in the operational band of spaceborne radar altimeter sensors and broadband RLANs (5.47 - 5.57 GHz) [17].

B. AXIAL RATIO

In order to obtain the measurements of the axial ratio, a reference antenna is used as a source while the polarization pattern of the antenna under test is recorded during its own rotation over the desired plane, Fig. 6. The polarization pattern is obtained with precision if it is guaranteed that the rate of azimuthal rotation of the reference antenna is much higher than the axial rotation rate of the test antenna positioner, so the first measures the polarization response at each direction before the test antenna moves to another angle. The recorded pattern is known as the axial ratio (AR) pattern [18], [20].

The polarization pattern of a circularly polarized antenna is 0 dB (axial ratio of unity). However, values under 3 dB have already been considered nearly circularly polarization. The measurement results of the axial ratio are presented in Fig.13, and they are satisfactory from 5 to 6 GHz.

C. RADIATION PATTERNS

For radar applications, the measured radiation patterns are very instructive. They are determined in the farfield region and represented as a function of the directional coordinates. The simulated and measured radiation patterns of the antenna in the YZ-plane at 5.5 GHz are shown in Fig.14, which exhibits right-hand circular polarization (RHCP) and left-hand circular polarization (LHCP) in the working band while exciting port 1 and port 2, respectively. The difference between the simulation results and measurement results is mainly due to the error of the instrument.

To measure the radiation pattern of the antenna in the anechoic chamber and to understand how this element behaves in the spacecraft, no remove before flight (RBF) pin is used. This RBF pin should be presented in a final integration of the circuitry and CubeSat power system, and be removed after the CubeSat is integrated into the flight dispenser.

IV. ANTENNA ARRAY SIMULATION AND MEASUREMENT RESULTS

Due to the radiation characteristics of single-element antennas, such as wide radiation pattern and low values of directivity, an antenna array of four elements was design to be integrated on a flat panel deployable wing of a CubeSat.

The antenna array is presented in Fig. 12, along with the anechoic chamber measurement environment. The interelement spacing, $L_{spacing}$, selected was according to [20]. This spacing is between half wavelength and one wavelength to prevent two scenarios: at least half wavelength is necessary so that the signals received from each antenna elements are considered independent in an uniform scattering

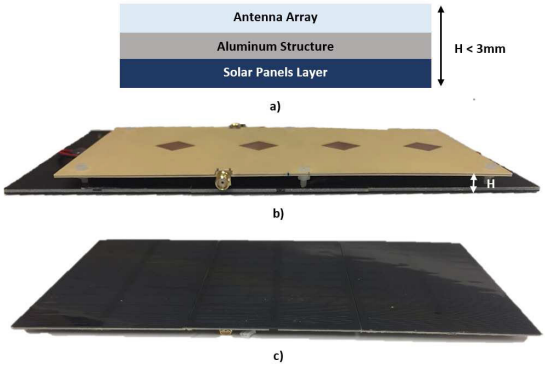

FIGURE 15. System representation: a) System layers schematic, b) antenna array side view, c) solar panels side view.

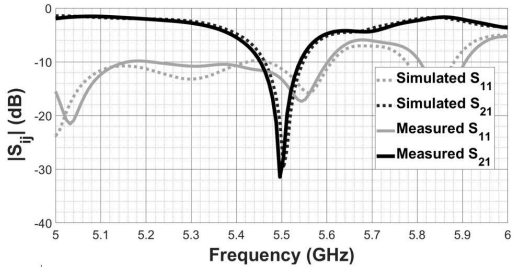

FIGURE 16. $|S_{ij}|$ simulation and measurement results.

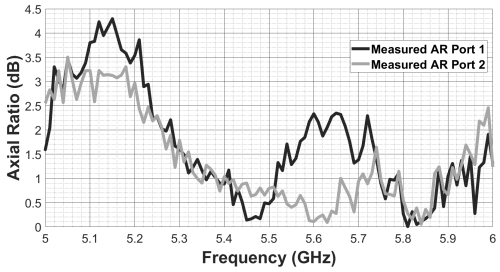

FIGURE 17. Measured axial ratio of the 4-element antenna array exciting Port 1 and Port 2 alternatively.

environment and no more than a wavelength so that grating lobes are avoided.

The hybrid coupler used in each element of the antenna array was the same as the single antenna element presented before so the separation between Port 1 and Port 2 was maintained, in order to keep similar results of isolation at 5.5 GHz. The final structure should include the antenna array, an aluminum structure, and solar panels. The representation of this arrangement is represented in Fig. 15.

A. RETURN LOSS AND ISOLATION

The return loss and isolation are obtained from the simulation and measurement of $|S_{11}|$ and $|S_{21}|$ of the antenna, Fig. 16. The antenna array suffered from a small shift of its center frequency targeted of 5.5 GHz of 10 MHz.

B. RADIATION PATTERNS AND AXIAL RATIO

The radiation patterns were obtained in the same conditions as the ones reported in section III.

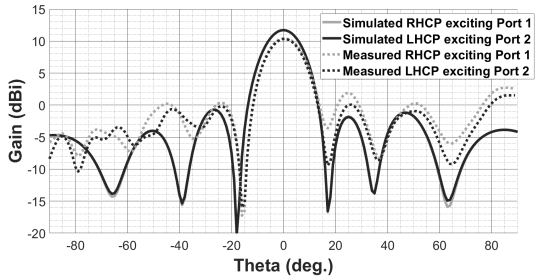

FIGURE 18. Simulation and measurement results of the radiation patterns show 12.4-dBi gain at 5.5GHz for the CP mode of the antenna array.

The AR obtained while exciting Port 1 and Port 2 alternatively is between 0.5 dB and 1 dB for 5.5 GHz, Fig. 17. The main difference between the implementation of this antenna array and the previous single element antenna is that the bandwidth where the antenna array is considered circularly polarized was reduced in 200 MHz. In Fig. 18, the radiation patterns in the YZ-plane at 5.5 GHz are displayed.

V. CONCLUSION

A dual CP antenna array arrangement for CubeSat SAR systems applications has been presented and measured. The experimental and simulated results are favorably matched, and the measurements of both designed elements show the capability and potential of an antenna array in a Tx/Rx communication system using the same center frequency with the lowest thickness reported. The presented work allows a new perspective on the designs that have been implemented, reporting new possibilities for the selected RF antenna elements. The development of the single element may be adapted with different feed arrangements due to its versatility, being the only condition a 90° phase difference between ports and isolation. The main contributions of this work are the study and implementation of new designs for antenna arrays aggregated with solar panels, which are one of the most advantageous and interesting solutions for the CubeSats' family. It would be pleasant to further develop different matching networks to obtain the same results using less space than the one a hybrid coupler occupies.

REFERENCES

[1] S. Gao and R. E. Hodges, "Advanced antennas for small satellites," *Proc. IEEE*, vol. 106, no. 3, pp. 391–401, Mar. 2018.
[2] Y. Rahmat-Samii, V. Manohar, and J. M. Kovitz, "For Satellites, Think Small, Dream Big: A review of recent antenna developments for CubeSats," *IEEE Antennas Propag. Mag.*, vol. 59, no. 2, pp. 22–30, Apr. 2017.
[3] Y. Rahmat-Samii and A. C. Densmore, "Technology trends and challenges of antennas for satellite communication systems," *IEEE Trans. Antennas Propag.*, vol. 63, no. 4, pp. 1191–1204, Apr. 2015.
[4] A. H. Lokman, P. J. Soh, S. N. Azemi, H. Lago, S. K. Podilchak, S. Chalermwisutkul, M. F. Jamlos, A. A. Al-Hadi, P. Akkaraekthalin, and S. Gao, "A review of antennas for picosatellite applications," *Int. J. Antennas Propag.*, vol. 2017, pp. 1–17, 2017.
[5] Y. Nakamura, K. Nishijo, N. Murakami, and K. Kawashima, "Small demonstration satellite-4 (SDS-4): Development, flight results, and lessons learned in JAXA's microsatellite project," in *Proc. 27th Annu. AIAA/USU Conf. Small Satell.*, Logan, UT, USA, Aug. 2013, pp. 1–15.
[6] R. Hodges, B. Shah, D. Muthulingham, and T. Freeman, "ISARA–integrated solar array and reflectarray mission overview," in *Proc. 27st Annu. AIAA/USU Conf. Small Satell.*, Logan, UT, USA, Aug. 2013.

[7] D. Pozar, "Wideband reflectarrays using artificial impedance surfaces," *Electron. Lett.*, vol. 43, no. 3, p. 148, 2007.
[8] N. Chahat, J. Sauder, M. Thomson, R. Hodges, and Y. Rahmat-Samii, "CubeSat deployable Ka-band mesh reflector antenna development for earth science missions," *IEEE Trans. Antennas Propag.*, vol. 64, no. 6, pp. 2083–2093, Jun. 2016.
[9] M. Maqsood, S. Gao, T. W. C. Brown, M. Unwin, R. De Vos Van Steenwijk, J. D. Xu, and C. I. Underwood, "Low-cost dual-band circularly polarized switched-beam array for global navigation satellite system," *IEEE Trans. Antennas Propag.*, vol. 62, no. 4, pp. 1975–1982, Apr. 2014.
[10] S. Padhi, N. Karmakar, C. Law, and S. Aditya, "A dual polarized aperture coupled circular patch antenna using a c-shaped coupling slot," *IEEE Trans. Antennas Propag.*, vol. 51, no. 12, pp. 3295–3298, Dec. 2003.
[11] M. J. Veljovic and A. K. Skrivervik, "Aperture-coupled low-profile wideband patch antennas for cubesat," *IEEE Trans. Antennas Propag.*, vol. 67, no. 5, pp. 3439–3444, May 2019.
[12] Q. Luo, L. Zhang, and S. Gao, "Wideband multilayer dual circularly-polarised antenna for array application," *Electron. Lett.*, vol. 51, no. 25, pp. 2087–2089, Dec. 2015.
[13] X.-Z. Lai, Z.-M. Xie, Q.-Q. Xie, and X.-L. Cen, "A dual circularly polarized RFID reader antenna with wideband isolation," *IEEE Antennas Wireless Propag. Lett.*, vol. 12, pp. 1630–1633, 2013.
[14] "CubeSat 101: Basic concepts and processes for first-time CubeSat developers," NASA, Washington, DC, USA, Tech. Rep., 2017.
[15] *Recommendation ITU-R M. 1653*, 2010.
[16] P. Sullivan and D. Schaubert, "Analysis of an aperture coupled microstrip antenna," *IEEE Trans. Antennas Propag.*, vol. AP-34, no. 8, pp. 977–984, Aug. 1986.
[17] D. Pozar, "A reciprocity method of analysis for printed slot and slot-coupled microstrip antennas," *IEEE Trans. Antennas Propag.*, vol. 34, no. 12, pp. 1439–1446, Dec. 1986.
[18] D. Pozar, "Microstrip antenna aperture-coupled to a microstripline," *Electron. Lett.*, vol. 21, no. 2, p. 49, 1985.
[19] D. M. Pozar, *Microwave Engineering*. Hoboken, NJ, USA: Wiley, 2012.
[20] C. Balanis, *Antenna Theory, Analysis, and Design*, 2nd ed. New York, NY, USA: Wiley, 1997.

PATRÍCIA BOUÇA (Member, IEEE) was born in Torres Novas, Portugal, in 1995. She received the master's degree in electronic and telecommunications engineering from the University of Aveiro, Portugal, in 2018, where she is currently pursuing the Ph.D. degree. Her research activities are supported by the Radio Systems Group, Institute of Telecommunications, Aveiro. Her current research interests include RF antenna systems for satellite communications and tunable microwave devices.

JOÃO NUNO MATOS (Member, IEEE) was born in Oliveira de Azeméis, Portugal, in 1959. He received the degree in electronic and telecommunications engineering from the University of Aveiro, Portugal, in 1982, the master's degree in electrical science from the University of Coimbra, Portugal, in 1989, and the Ph.D. degree in electrical engineering from the University of Aveiro, in 1995. He worked twice in the industry, from 1982 to 1983, with Portugal Telecom Innovation, Aveiro, Portugal, and in 1990, with Ensa Electronic, Madrid, Spain. From 1998 to 2000, he was the Head of the Electronics and Telecommunications Department, Aveiro University, Portugal. He is currently an Associate Professor with the University of Aveiro and a Senior Researcher with the Telecommunications Institute. He is author or coauthor of more than 100 international conference papers and journals articles. With the Telecommunications Institute, he participated or led dozens of research's projects in RF/microwave (MW) circuits, system design, and system integration. His current topics of interest are satellite communications and radars with a special focus on front-end and smart antennas, and engineering education. He is a member of several scientific committees of conferences and journals, as well as professional organizations. He is also on the Executive Committee of the IEEE Portugal Education Chapter (the 2019 IEEE Education Society Chapter Achievement Award).

SÉRGIO REIS CUNHA was born in Porto, Portugal, in 1968. He received the bachelor's degree, M.Sc., and Ph.D. degrees in electric and computers engineering from the University of Porto, Portugal, in 1991, 1994, and 2001, respectively. He is currently an Assistant Professor with the Department of Electric and Computers Engineering, University of Porto. His research interests cover a broad spectrum related to signal processing, from the field of control systems (the M.Sc. and Ph.D. degrees area) to navigation, telecommunications, and remote sensing, including synthetic aperture systems. In the field of telecommunications, he has been developing signals to support both communications and remote sensing applications. He has also been involved in the development of Synthetic Aperture Radar based on a Software Defined Radio platform in the development of which he also participated. As a related interest, he is also involved in antenna design.

NUNO BORGES CARVALHO (Fellow, IEEE) was born in Luanda, Angola, in 1972. He received the Diploma and Ph.D. degrees in electronics and telecommunications engineering from the University of Aveiro, Aveiro, Portugal, in 1995 and 2000, respectively.

He is currently a Full Professor and a Senior Research Scientist with the Institute of Telecommunications, University of Aveiro. He has coauthored *Intermodulation Distortion in Microwave and Wireless Circuits* (Artech House, 2003), *Microwave and Wireless Measurement Techniques* (Cambridge University Press, 2013), and *White Space Communication Technologies* (Cambridge University Press, 2014). He has been a Reviewer and the author of more than 200 articles in magazines and conferences. He is the Editor-in-Chief of the *Cambridge Wireless Power Transfer Journal*, an Associate Editor of the *IEEE Microwave Magazine* and a former Associate Editor of the IEEE TRANSACTIONS ON MICROWAVE THEORY AND TECHNIQUES and *IET Microwaves Antennas and Propagation Journal*. He is the co-inventor of six patents. His main research interests include software-defined radio front-ends, wireless power transmission, nonlinear distortion analysis in microwave/wireless circuits and systems, and the measurement of nonlinear phenomena. He has recently been involved in the design of dedicated radios and systems for newly emerging wireless technologies.

Dr. Carvalho is a member of the IEEE MTT ADCOM, the Past-Chair of the IEEE Portuguese Section, MTT-20 and MTT-11, and also belong to the technical committees, MTT-24, and MTT-26. He is also the Vice-Chair of the URSI Commission A (Metrology Group). He was a recipient of the 1995 University of Aveiro and the Portuguese Engineering Association Prize for the Best 1995 student at the University of Aveiro, the 1998 Student Paper Competition (Third Place) of the IEEE Microwave Theory and Techniques Society (IEEE MTT-S) International Microwave Symposium (IMS), and the 2000 IEE Measurement Prize. He is a Distinguished Microwave Lecturer for the IEEE Microwave Theory and Techniques Society.